LRP 591/97 November 1997

# PRESSURE AND CONDUCTIVITY PROFILES IN OHMIC TCV DISCHARGES

H. Weisen, R. Behn, I. Furno,
J.-M. Moret & O. Sauter

submitted for publication to
Plasma Phys. & Contr. Fusion

# Pressure and conductivity profiles in ohmic TCV discharges

H. Weisen, R. Behn, I. Furno, J.-M. Moret and O. Sauter

Centre de Recherches en Physique des Plasmas
Association EURATOM - Confédération Suisse
École Polytechnique Fédérale de Lausanne
CH-1015 Lausanne, Switzerland

**Abstract.**

A large variety of plasma conditions has been created in TCV (Tokamak à Configuration Variable, $B_T$<1.5T, $R_0$=0.88m, a<0.25m). They include elongations in the range 1 to 2.58, triangularities between -0.7 and 1 as well as 'square' shapes and plasma currents in the range 0.1-1MA. Over the entire range of quasi-stationary ohmic conditions investigated we observe a correlation between electron pressure profiles and conductivity profiles, suggesting that $\langle p \rangle / p(0) = \langle j \rangle / j(0)$, where <> refers to an average over the volume or respectively the cross sectional area of the plasma. The profiles become broader as the average current density is increased. These "profile consistency" features are apparent agreement with theoretical considerations based on minimum energy states of the plasma or on stationary entropy. Further analysis of the experimental evidence, together with a simple model of the current profile based on marginal stability to the internal kink mode in the core and neoclassical conductivity in the confinement zone, however shows that the observations can be accounted for by the effects of sawtooth activity.

## 1.0 Introduction

Experimental observations and theoretical models supporting the idea that electron temperature and more so the pressure and/or current density in tokamaks assume certain privileged profile shapes have been reported for more than two decades [TFR group 1975, Coppi 1981, Biskamp 1986, Kadomtsev 1987, Arunasalam 1990, Minardi (et al) 1990, 1997]. Some observations, such as [Gruber et al 1987] suggest that the plasma pressure profile rather than the temperature

profile is most resilient to changes in plasma conditions such as confinement mode or heating. The basic idea is that plasmas with ohmic heating only or with weak additional heating plasma profile assume a class of shapes depending only on the plasma safety factor $q_a$. In some theories a relationship between relaxed current and pressure profiles is derived from a variational principle such that the magnetic [Biskamp 1986] energy or the total energy [Kadomtsev 1987], is minimized for a given plasma current, leading for plasmas with circular cross section to similar current and pressure profiles of the form $j=j(0)(1+q_a\rho^2)^{-2}$ and $p=p(0)(1+q_a\rho^2)^{-2}$, where $\rho=r/a$ is the normalized minor radius. A similar strong relationship is predicted by maximum entropy configurations [Minardi and Lampis 1990, Minardi 1992, 1997], where the requirement of stationary entropy, together with the equilibrium equation leads to a pressure profile such that $p \propto \Psi$, where $\Psi$ is the poloidal flux and is essentially proportional to the flux surface averaged current density. These authors also assume Spitzer conductivity ($\sigma_{Spit} \propto T_e^{3/2}$) to temptatively infer relations between temperature and pressure, repectively density profiles. Such relations, e.g. $\langle p_e \rangle / p_e(0) = \langle T_e^{3/2} \rangle / T_e^{3/2}(0)$, where the brackets indicate a volume (or practically equivalently cross sectional area) averages, are indeed observed over a wide range of plasma shapes in ohmic L-modes in TCV as reported earlier [Weisen et al 1997a] and shown in figure 1 for a wider range of plasma shapes including elongations up to 2.54, triangularities in the range -0.5 to +0.7, 'square' and 'rhomboidal' shapes and diverted L-mode plasmas [Weisen et al 1997b]. The measurements were obtained with a multichord Thomson scattering system [Behn et al 1995] with 10-25 measurement locations in the plasma depending on plasma size and mapped onto the flux contours calculated using the equilibrium reconstruction code LIUQE [Hofmann et al 1988] for calculation of the relevant averages. The width of the pressure or conductivity profiles increases approximately as $1/q_{95}$ (fig.2), in qualitative agreement with the minimum energy models above. Note that the most elongated plasmas have so far only been produced in a narrow range of $q_{95}$ as a result of limitations due to vertical stability and kink instability [Hofmann 1997b]. Experimentally a broadening of plasma profiles with $1/q_a$ has been observed already in early tokamak experiments [TFR Group 1975]. This, together with the observed broadening of the sawtooth inversion radius with $1/q_a$, led to the postulation of the "principle of profile consistency" [Coppi 1980].

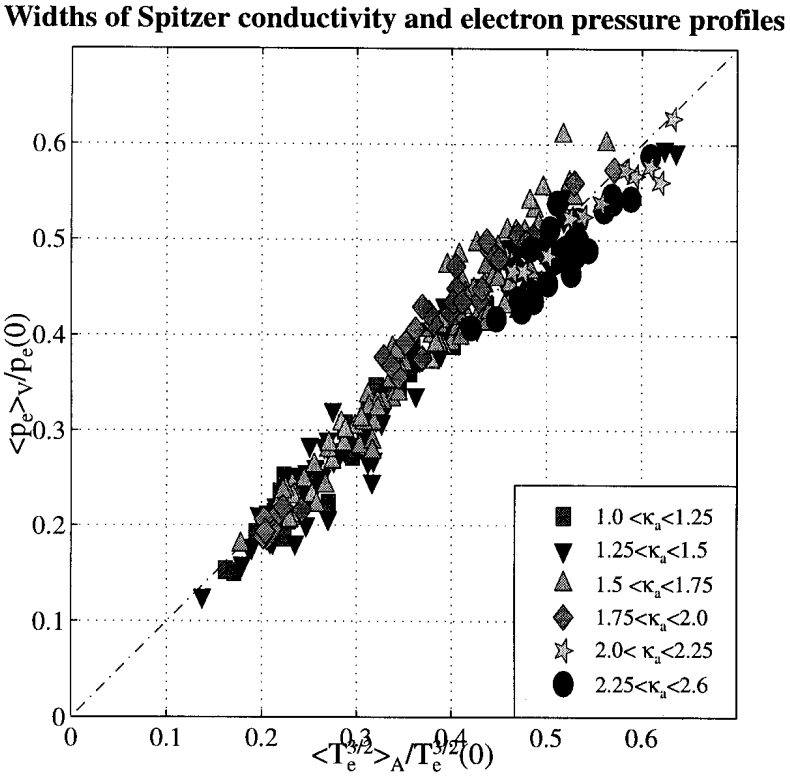


*Fig. 1 Relationship between widths of Spitzer conductivity and electron pressure profiles. The symbols refer to classes of elongation.*

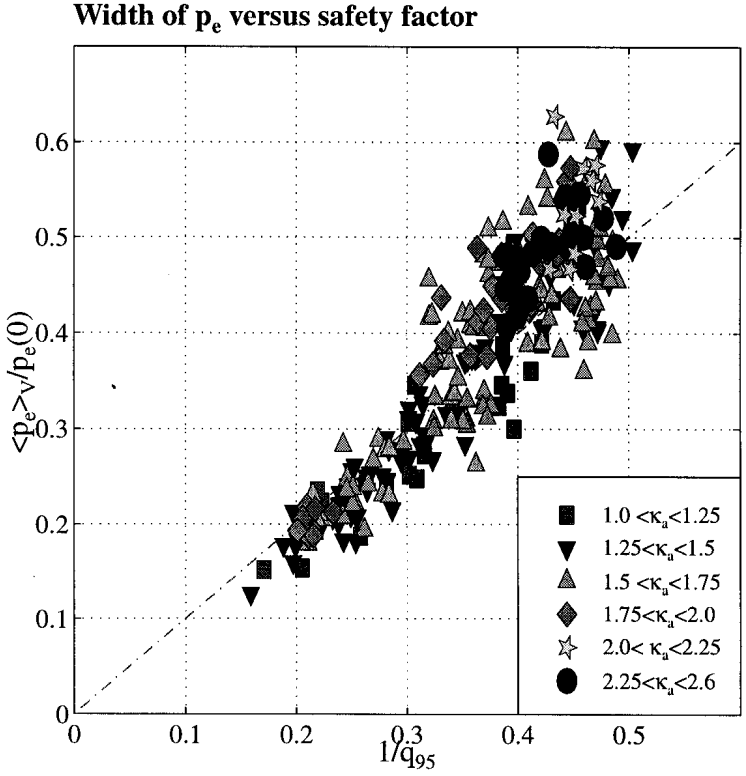


*Fig. 2 Width of electron pressure profiles versus safety factor at 95% of the poloidal flux.*

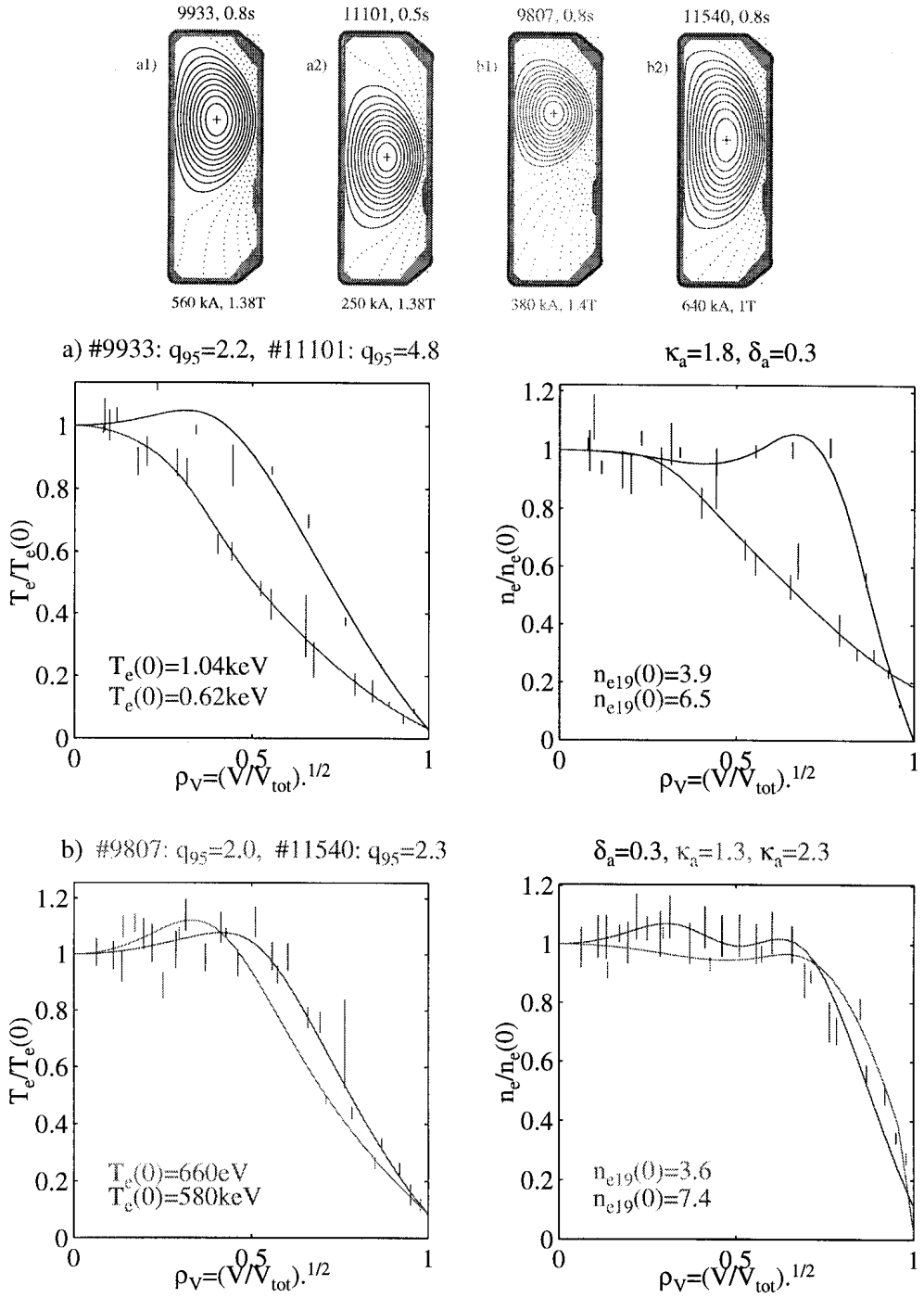


*Fig. 3 Electron temperature (left) and density profiles (right) for different plasma conditions*
*a1) & a2) configurations corresponding to subplot a)*
*b1) & b2) configurations corresponding to subplot b)*

Inspection of the profiles of electron temperature and density in fig. 3 illustrates some of these features in selected configurations. In fig.3a we show $T_e$ (left) and $n_e$ (right) profiles for two discharges having the same shape as shown in fig.3a1 and a2, but which differ by more than a factor of 2 in $q_{95}$ and have profiles of different broadness. The profiles are shown as a function

of an effective minor radius defined as $\rho=(V/V_{tot})^{1/2}$ where V is the volume enclosed within the flux surface considered and $V_{tot}$ is the total plasma volume. Conversely plasmas with very different elongations (fig.3b1 & b2), but similar values of $q_{95}$ or of average current density have similar profiles (fig.3b). Also density profiles are systematically broader, by a factor of 1.3 on average, than temperature profiles (fig.4), independently of the absolute value of density, which may seem surprising since neutral penetration in these gas-fuelled plasmas depends on density. The observation of broader density profiles seems in qualitative agreement with prediction of the theories mentioned above if the $T_e^{3/2}$ profile shape is assumed to be a reflection of the current profile shape and is suggestive of some form of coupling between particle and energy transport.

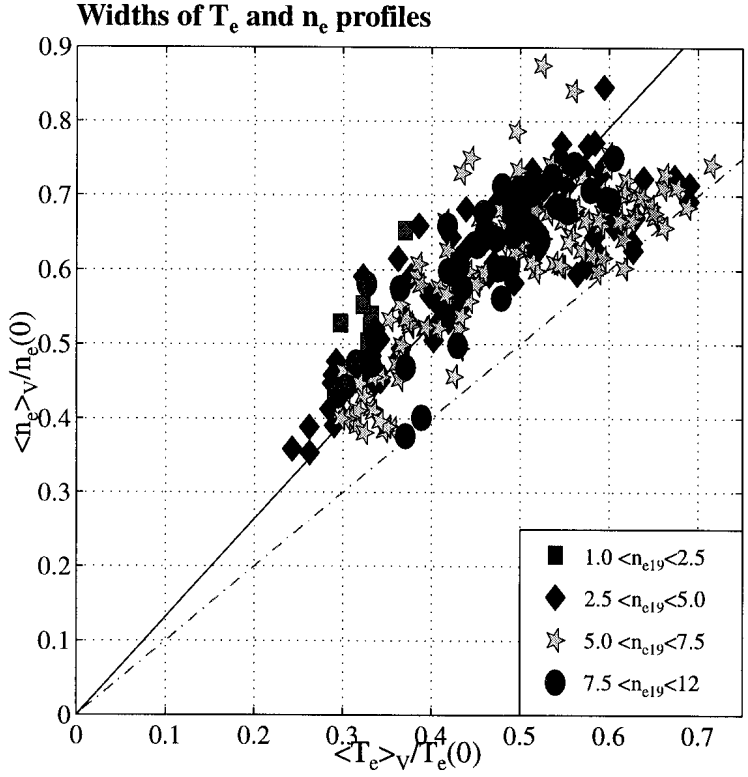


*Fig. 4 Widths of electron density profile versus width of electron temperature profile. The different symbols refer to classes of line average electron density.*

## 2.0 "Neoclassical" current profile limited by q≥1

The main criticism of taking the $T_e^{3/2}$ profile as a reflection of the current profile is that conductivity in a tokamak configuration departs sharply from Spitzer conductivity due to friction of the current carrying passing electrons with trapped electrons. But even the neoclassical conduc-

tivity $\sigma_{neo}$ [Hirshmann and Sigmar 1981] profile alone provides an unsatisfactory (excessively peaked) model of the current profile. The reason for this is that a sawtoothing tokamak, although quasi-stationary on average, is never in resistive equilibrium. The well known sawtooth cycle comprises a ramp phase during which current diffuses towards the core, followed by a rapid relaxation when the current and energy accumulated during the ramp phase are expelled from within the sawtoothing core defined by the sawtooth inversion radius. Since sawtooth periods in ohmic plasmas are much shorter ($< 10^{-2}$ s in TCV) than current diffusion times ($\sim 10^{-1}$ s for the plasma core) the core remains far from resistive equilibrium and the current profile must be expected to be different from the conductivity profile. Another concern is the applicability of the above theories to plasmas dominated by gross MHD phenomena, such as sawteeth, which are a hallmark of "normal" ohmic discharges and are governed by MHD stability criteria not contained in their basic assumptions.

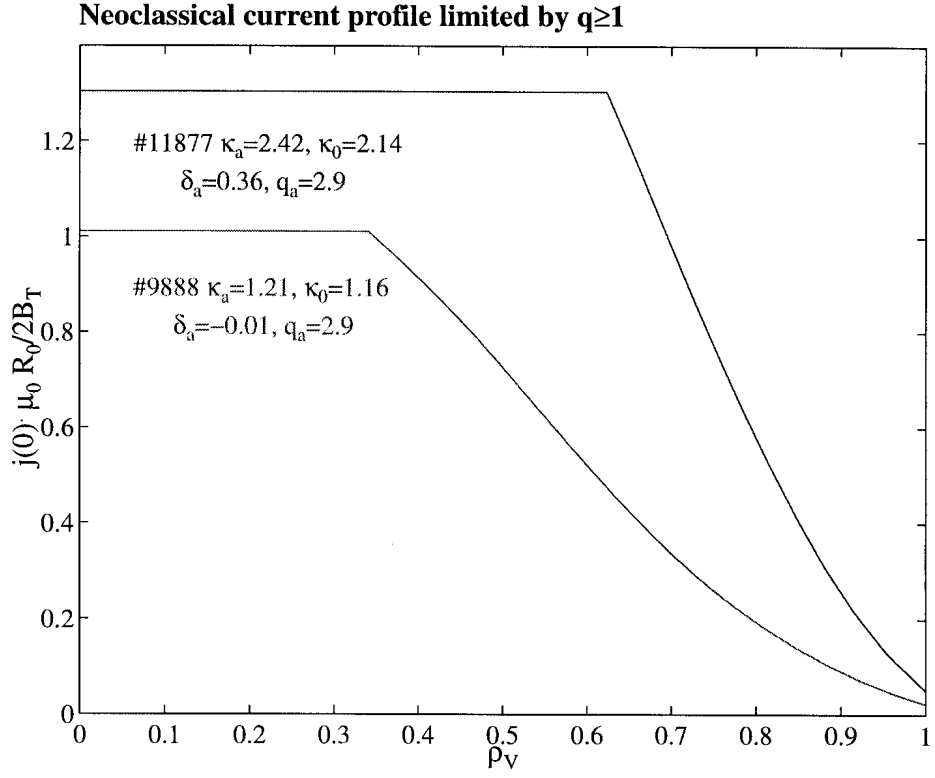


*Fig. 5 Examples of model current profiles*

We therefore propose a temptative model current profile given as $j=E\sigma_{neo}+j_{boot}$ outside the sawtoothing zone and by $j= j_0 = \frac{(\kappa_0 + 1/\kappa_0)B_0}{\mu_0 R_0 q_0}$ in the plasma core. The subscript 0 refers to

values at the magnetic axis of the discharge, E is the externally induced electric field and $j_{boot}$ is the bootstrap current, which in these ohmic plamas only contributes a few percent to the total current. We take $q_0=1$ in accordance with marginal stability with respect to the internal m=1, n=1 kink mode [Bussac et al 1975]. Fig.5 shows two examples from the database with the same value of the safety factor at the boundary, but different core elongations, as indicated in the figure. The neoclassical expressions were taken from Sauter [1996,1994] and the trapped electron fraction was obtained from a formulation by Lin-Liu and Miller [1995]. Although generally in good agreement we did not use the absolute values of $E\sigma_{neo}$ because of uncertainties in $Z_{eff}$, but rescaled $E\sigma_{neo}$ such that $\int j dA = I_p$. This normalization leads to the determination of extent of the central flat current zone, which can be cross-checked with the sawtooth inversion radius determined using X-ray tomography.

## 3.0 Sawtooth inversion radius from X-ray tomography

TCV is equipped with an X-ray tomography system comprisising 200 viewing lines in 10 cameras, fig.6 (left). Tomographic inversions for the data shown were obtained using the Minimum Fisher Regularization method on a pixel grid with 3.8cm resolution. Time sequences of inverted signals of typically 10 ms duration, comprising 2-3 sawtooth crashes, were then analysed using the Singular Value Decomposition method to yield the spatial structures (*topos*) and corresponding time evolution (*chronos*) [Anton et al 1996]. Low order structures ($m\leq3$) are clearly identifiable, including two m=0 components from which the inversion contour is reconstructed [Furno et al 1997]. Fig 6 (right) shows examples from four discharges with the same average density, elongation and edge safety factor, but different triangularity. The top traces are raw x-ray signals from detectors viewing the plasma core and show sawtoothing and superimposed MHD mode activity (mainly m=1). The lower subplots show the inversion contour and the last closed flux surface. An advantage of the SVD-based method is that inversion contours can be determined even in the presence of very weak sawtooth activity and strong m>0 modes, as frequently observed at negative triangularity and low average current density.

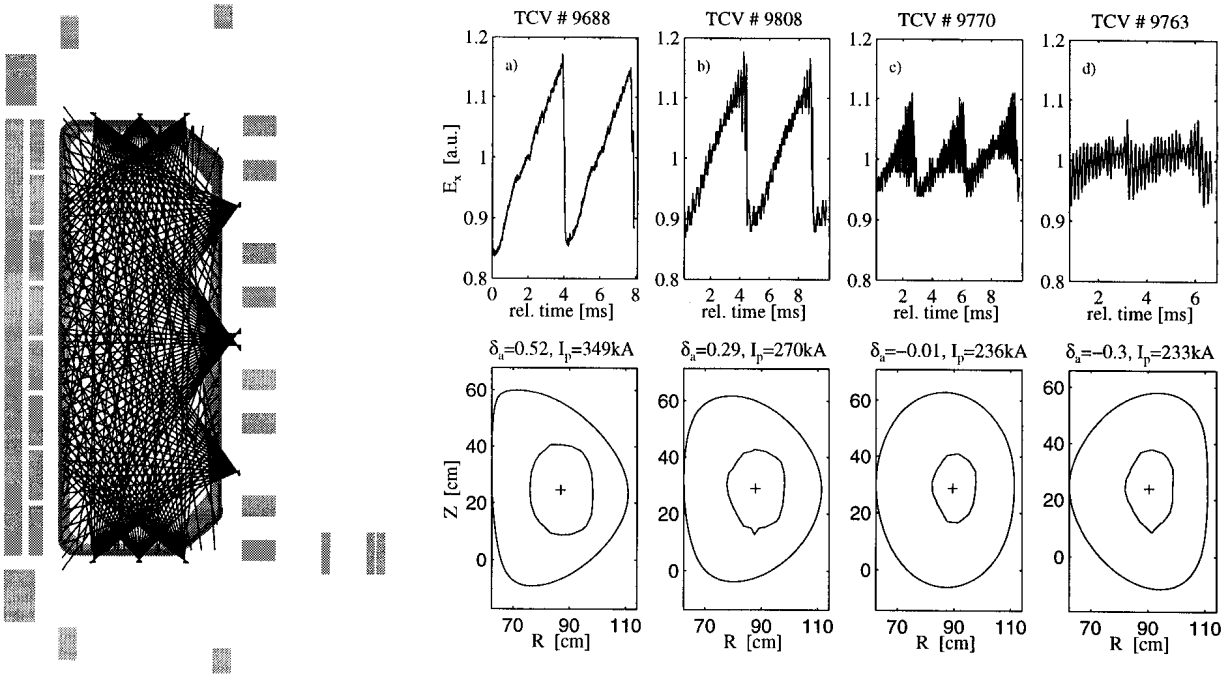


*Fig. 6 X-ray tomography on TCV. Left: Geometry of X-ray cameras. Right: Examples of raw X-ray signals (top) and sawtooth inversion contours (bottom) in a triangularity scan.*

A empirical scaling of sawtooth inversion radius, based on discharges with elongations up to 1.9, has previously been given as $\rho_{inv} \approx \langle j \rangle^*/2$, where $\langle j \rangle^*$ is the dimensionless average current density $\mu_0 R_0 I_p / A B_0$, with A is the cross-sectional area enclosed within the last closed flux surface [Weisen et al 1997a]. For extreme elongations this scaling becomes unsatisfactory because of the increased current carrying capacity of the core, as illustrated in fig.5. This effect is however readily accounted for by a corrective factor proportional to $(\kappa_0 + 1/\kappa_0)^{-1}$. In fig.7 we show the measured effective inversion radius as a function of the proposed scaling expression, $1.24\langle j \rangle^*/(k+1/k)$, where $k = 1 + 0.8(\kappa_a - 1) \approx \kappa_0$ is an approximate expression for the core elongation based on the externally controlled boundary elongation. The proposed expression can be viewed as an extension to arbitrary shape and elongation of the corresponding scaling for circular tokamaks, $\rho_{inv} \approx 1/q_a$ [Arunasalam et al, 1988]. Physically these scalings are however not entirely satisfactory since they predict a vanishing inversion radius only for a vanishing normalized plasma current.

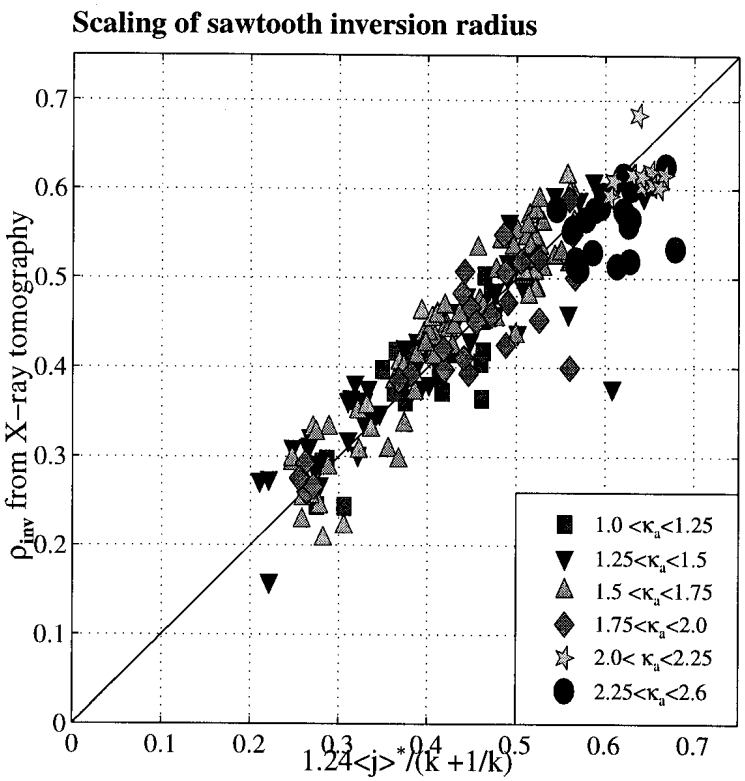


*Fig. 7 Scaling of inversion radius for arbitrary shape and elongation.*

# 4.Discussion

The measured inversion radii are in good agreement with the radii of the flat core region from the current profile model in section 2, as shown in fig.8. Let's note that the value of the safety factor in the plasma core, which is difficult to measure, has been a matter of controversy for more than a decade. While some experiments have reported $q_0$ profiles which are flat in the core region with magnitudes very close to unity, other experiments have reported values of $q_0$ significantly below unity [Soltwisch 1992] and therefore not consistent with the model proposed above. If we choose $q_0$=0.8, as is typical of many of the latter, the modelled q=1 surface falls short of the measured inversion radius by typically 0.15 minor radii and even vanishes in some cases when sawteeth are observed. The importance of the sawtooth inversion radius for determining the width of the pressure profile can be appreciated from fig. 9.

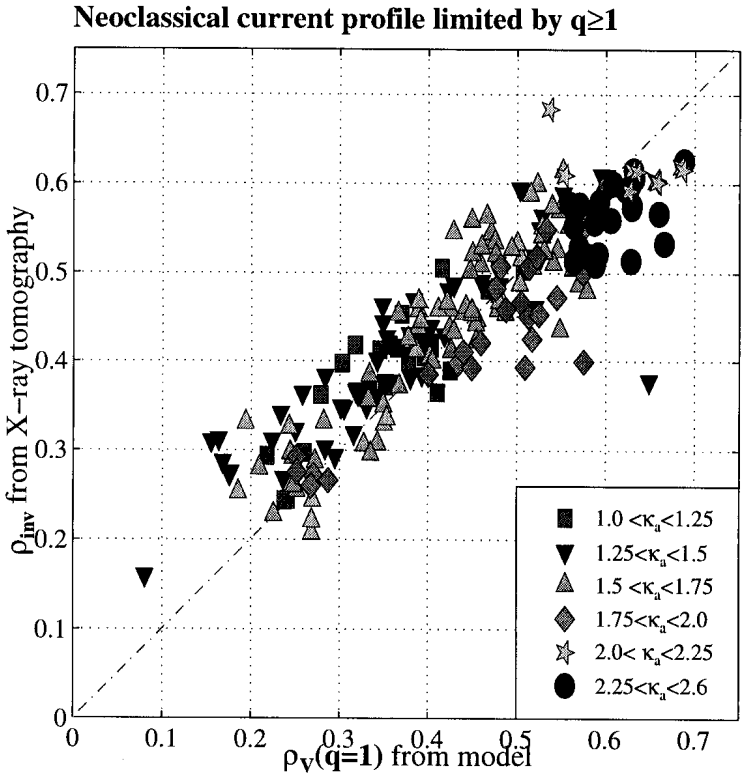


*Fig. 8 Measured inversion radius versus outermost q=1 surface from current profile model*

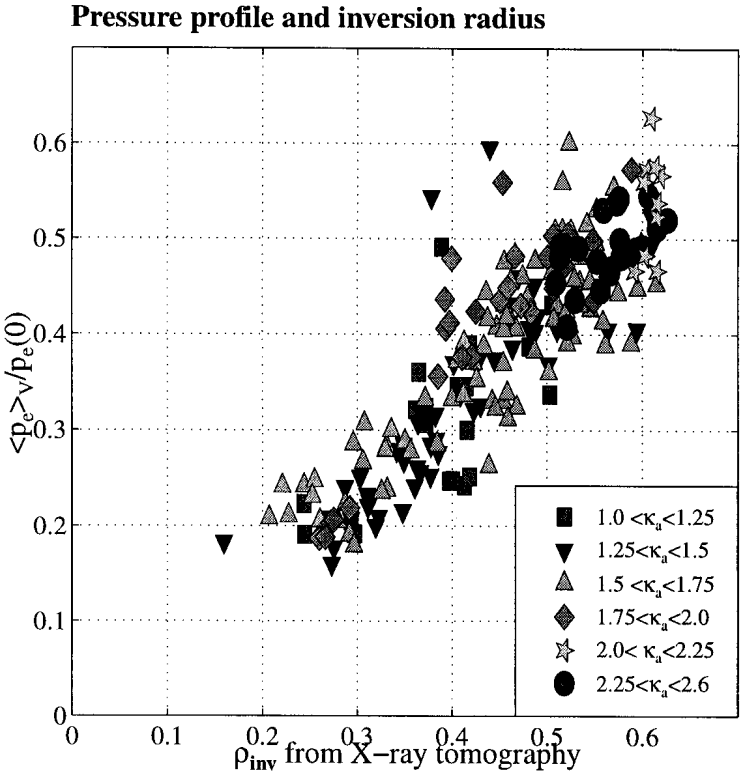


*Fig. 9 Width of electron pressure profile versus inversion radius.*

The electron pressure profile width remains proportional to that of the model profile, although the model current profile is slightly broader, by an average factor of 1.2, than the electron pressure profile from Thomson scattering (fig.10). The total pressure profile however may be somewhat broader than the electron pressure profile if the ion temperature profile which is not (yet) measured on TCV is very broad. Such a relationship is not surprising since both the current and the pressure profile must be expected to be flattened in the plasma core, at least when, as in TCV, the sawtooth period is substantially shorter (<10 ms) than both the energy confinement time (10-60 ms) and the skin time (~100 ms). The resulting profiles are hence more or less trapezoidal with similar widths, irrespectively of their detailed shapes, which depend on transport. To illustrate this we have plotted the widths of two model pressure profiles, one trapezoidal and one trapezoidal squared, (with a flat core region of the same extent as that of the model current profile) versus the widths of the model current profile for all data points (fig 11). This lack lack of sensitivity of profile "consistency features" to transport in the confinement zone is also borne out by an evaluation of several transport models by Arunasalam et al [1988]. The greater width of the density profiles is likely to be due to the fact that the source of the particles is peripheral, rather than localized at the plasma core as is the case of the ohmic power. The relatively strong peaking observed at low current densities (fig3.a) and the lack of a density dependence of the broadness (fig.4) however indicate the existence another transport mechanism, such as a particle pinch. The only coupling between particle and energy transport which can be inferred from the results presented here is the existence of a shared mechanism of flattening of the core profiles, namely sawtooth activity.

The conclusion hence is that profile relations such as $\langle j\rangle/j_0 \approx \langle p\rangle/p_0$ are consequences of core profile flattening resulting from sawtooth activity and are fairly insensitive to the detailed physics governing transport in the confinement zone. The observations reported here and previously can therefore not be considered as supportive of the theories mentionned in the introduction. To be fair, the predictions of these theories should be compared to experimental results from discharges which are exempt of gross MHD activity. Such discharges may be difficult to produce since the disappearance of sawteeth often coincides with the onset of strong m>0 mode activity. In TCV ohmic discharges sawteeth are observed at least up to $q_{95}=6.5$. The "profile consistency" features observed in sawtoothing discharges thus appear to be the result of the combined effects of marginal stability to the internal kink mode in the plasma core and neoclassical conductivity in the confinement zone.

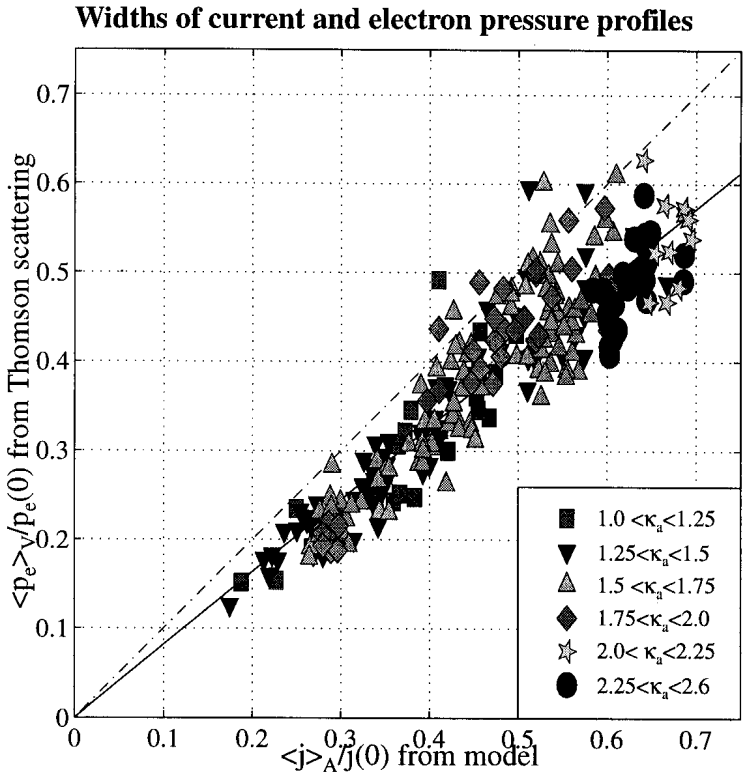


*Fig. 10 Pressure profile width versus width of model current profile*

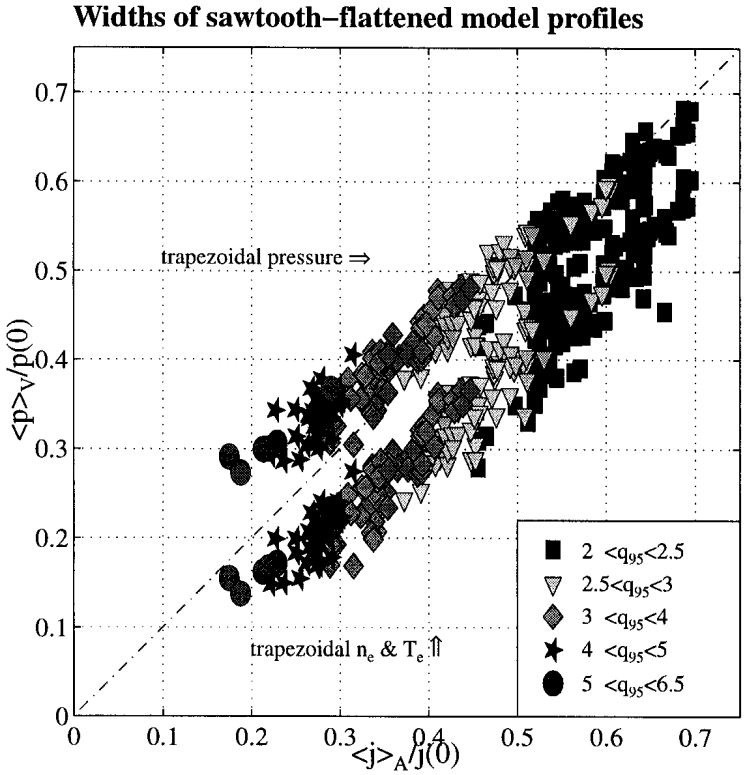


*Fig. 11 Width of two different model pressure profiles versus width of model current profile*

**Acknowledgements:** This work was partly supported by the Swiss National Foundation for Scientific Research. Helpful discussions with E. Joffrin and E. Minardi are acknowledged.

**References:**

Anton M., Weisen H., M.J. Dutch, *Plasma Phys. Control. Fusion* **38** (1996) 1849

Arunasalam V. et al, *Nuclear Fusion* **30** (1988), 2111

Behn R., Z.A. Pietrzyk Z.A., Anton M. et al, Proc 7th Int Symp Laser Aided Plasma Diagnostics, Fukuoka, Japan 5-8 Dec 1995, page 392 (edited by K. Muruoka)

Biskamp D., *Comments Plasma Phys. Control. Fusion* 10, (1986) 165

Bussac M.N., Pellat R., Edery D. and Soule J.L, *Phys. Rev. Lett.* **35** (1975), 1638

Coppi B. *Comments Plasma Phys. Controlled Fusion* **5** (1980) 261

Furno I., Weisen H., Moret J.M et al, 24th EPS on Controlled Fusion Plasma Physics, *ECA* **21A** (1997), part II, 545

Gruber O. et al, 14th EPS on Controlled Fusion Plasma Physics, *ECA* **11D** (1987), part I, 45

Hirshman S.P. and D.J. Sigmar, *Nuclear Fusion* **21** (1981) 1079

Hofmann F. and Tonetti G., *Nuclear Fusion* **28** (1988) 1871

Hofmann F., Behn R., M.J. Dutch et al, 24th EPS on Controlled Fusion Plasma Physics, *ECA* **21A** (1977), part II, 525

Kadomtsev B., Proc. *International Conference on Plasma Physics,* Kiev, 6-12.4 (1987), 1273, edited by A.G. Sitenko, published by World Scientific

Lin-Liu Y.R and Miller R.L., Physics of Plasmas **2**,(1995), 1666

Minardi E. and Lampis G., *Plasma Phys. Contr. Fusion* **32** (1990) 819

Minardi E. *report FP* 97/3, Istituto di Fisica del Plasma, Via Bassini 15, I-20133 Milano (1997)

Sauter O., *Theory of Fusion Plasmas* Lausanne-Varenna Int. Workshop (1994) p 337

Sauter O., *ITER EDA memo* IDoMS No s19 MD 18 96-08-06 F1 (1996)

Soltwisch H., *Plasma Physics and Controlled Fusion* **34** (1992) 1669 and references therein

TFR Group, presented by D. Launois, *Proc 7th European Conf. Contr. Fusion and Plasma Phys.*, (Lausanne 1-5 Sept. 1975) Vol II, 1

Weisen H. et al, (and refs. therein) to be published in *Nuclear Fusion*, available from the authors as *report LRP* 571/97 (1997a)

Weisen H. et al, invited paper at the 24th EPS on Controlled Fusion Plasma Physics (1997b), to be published in *Plasma Physics Contr. Fusion* available as *report LRP 577/97*